Virology 379 (2008) 125–134

Contents lists available at ScienceDirect

Virology

journal homepage: www.elsevier.com/locate/yviro

Primary HIV-1 R5 isolates from end-stage disease display enhanced viral fitness in parallel with increased gp120 net charge

Johanna Repits [a], Jasminka Sterjovski [b,c], Daniel Badia-Martinez [d], Mattias Mild [a,e,i], Lachlan Gray [b,f], Melissa J. Churchill [b,c], Damian F.J. Purcell [f], Anders Karlsson [g], Jan Albert [h,i], Eva Maria Fenyö [a], Adnane Achour [d], Paul R. Gorry [b,c,f,*,1], Marianne Jansson [a,h,i,*,1]

[a] Department of Laboratory Medicine, Lund University, Sweden
[b] Macfarlane Burnet Institute for Medical Research and Public Health, Melbourne, Australia
[c] Department of Medicine, Monash University, Melbourne, Australia
[d] Center for Infectious Medicine, Karolinska Institutet, Karolinska University Hospital Huddinge, Stockholm, Sweden
[e] Department of Experimental Medical Science, Lund University, Sweden
[f] Department of Microbiology and Immunology, University of Melbourne, Australia
[g] Department of Infectious Medicine, South Hospital, Stockholm, Sweden
[h] Department of Microbiology, Tumor and Cell Biology, Karolinska Institutet, Stockholm, Sweden
[i] Department of Virology, Swedish Institute for Infectious Disease Control, Solna, Sweden

ARTICLE INFO

Article history:
Received 11 April 2008
Returned to author for revision
28 April 2008
Accepted 11 June 2008
Available online 30 July 2008

Keywords:
HIV-1
R5
AIDS
Env
gp120
Net charge
Evolution
Viral fitness

ABSTRACT

To better understand the evolution of the viral envelope glycoproteins (Env) in HIV-1 infected individuals who progress to AIDS maintaining an exclusive CCR5-using (R5) virus population, we cloned and sequenced the *env* gene of longitudinally obtained primary isolates. A shift in the electrostatic potential towards an increased net positive charge was revealed in gp120 of end-stage viruses. Residues with increased positive charge were primarily localized in the gp120 variable regions, with the exception of the V3 loop. Molecular modeling indicated that the modifications clustered on the gp120 surface. Furthermore, correlations between increased Env net charge and lowered $CD4^+$ T cell counts, enhanced viral fitness, reduced sensitivity to entry inhibitors and augmented cell attachment were disclosed. In summary, this study suggests that R5 HIV-1 variants with increased gp120 net charge emerge in an opportunistic manner during severe immunodeficiency. Thus, we here propose a new mechanism by which HIV-1 may gain fitness.

Introduction

The reverse transcriptase enzyme of human immunodeficiency virus type 1 (HIV-1) has a low fidelity and lacks proof-reading capacity. This results in a high mutation rate of approximately one point mutation per genome per replication cycle (Mansky and Temin, 1995). Consequently, within an infected individual viral quasispecies of distinct but closely related viruses are established. With 10^{10} new virions produced every day in combination with the high mutation rate, the quasispecies population is very variable (Perelson et al., 1996). In constant interplay with selective forces of the host and therapeutic agents, the quasispecies population evolves continuously during the course of infection (van Opijnen and Berkhout, 2005). Thus, the intra host virus evolution can be traced by analyzing the changes in the viral genome over time.

The viral envelope gp120/gp41 trimeric complex (Env), which is physically exposed to the host immune system has been shown to exhibit the greatest genetic diversity among the HIV-derived proteins (Hahn et al., 1985). Previous studies have revealed correlations between variations in the gp120 sequence and the function of the virus. Mutations in the variable loops (V1, V2 and V3) of gp120, resulting in length variations and charge differences, are related to altered cell tropism (Hoffman and Doms, 1999).

* Corresponding authors. P.R. Gorry is to be contacted at Macfarlane Burnet Institute for Medical Research and Public Health, GPO Box 2284, Melbourne 3001, Victoria, Australia. Fax: +61 3 9282 2100. M. Jansson, Swedish Institute for Infectious Disease Control, Nobelsvag 18, 171 82 Solna, Sweden. Fax: +46 8337460.
E-mail addresses: johanna.repits@med.lu.se (J. Repits), jasminka@burnet.edu.au (J. Sterjovski), Daniel.Badia-Martinez@ki.se (D. Badia-Martinez), Mattias.Mild@med.lu.se (M. Mild), lachlang@burnet.edu.au (L. Gray), churchil@burnet.edu.au (M.J. Churchill), dfjp@unimelb.edu.au (D.F.J. Purcell), anders.karlsson@sodersjukhuset.se (A. Karlsson), jan.albert@smi.se (J. Albert), Eva_Maria.Fenyo@med.lu.se (E.M. Fenyö), Adnane.Achour@ki.se (A. Achour), gorry@burnet.edu.au (P.R. Gorry), marianne.jansson@smi.se (M. Jansson).
[1] These authors contributed equally to this work.

0042-6822/$ – see front matter © 2008 Elsevier Inc. All rights reserved.
doi:10.1016/j.virol.2008.06.014

To gain entry into target cells HIV-1 binds to CD4 via the viral glycoprotein gp120 which initiates a series of events including binding of a coreceptor, CCR5 and/or CXCR4, and ultimately gp41-mediated fusion of the viral and cell membranes (Pierson and Doms, 2003). CCR5-restricted (R5) viruses predominate in early, asymptomatic stages of infection (van't Wout et al., 1994). Emergence of viruses able to use CXCR4 instead of- or in addition to CCR5 for cell entry has been correlated to rapid progression to AIDS (Bjorndal et al., 1997). However, approximately 50% of infected individuals progress to AIDS while maintaining exclusive use of CCR5 (de Roda Husman et al., 1999; Jansson et al., 1999; Karlsson et al., 1994; Koot et al., 1993). We and others have previously described late stage R5 HIV-1 variants, isolated from AIDS patients, with altered biological properties compared to viruses isolated before AIDS onset (Gorry et al., 2005; Gray et al., 2005; Jansson et al., 1999; Jansson et al., 1996; Karlsson et al., 2004; Koning et al., 2003; Kwa et al., 2003; Repits et al., 2005; Sterjovski et al., 2007). Our previous studies on sequential R5 isolates obtained before and after AIDS onset revealed an evolution of the R5 phenotype with respect to enhanced viral fitness, altered mode of coreceptor use and reduced sensitivity to inhibition by CCR5 ligands and HIV-1 entry inhibitors (Gray et al., 2005; Jansson et al., 1999; Jansson et al., 1996; Karlsson et al., 2004; Repits et al., 2005; Sterjovski et al., 2007).

In the present study we sought to better understand the evolution of the HIV-1 R5 envelope of primary isolates during disease progression. Multiple full-length gp160 *env* sequences from R5 isolates, obtained before and after AIDS onset, were analyzed. We demonstrate the emergence of R5 variants with gp120 molecules that display an increased positive net charge at the end-stage HIV-1 infection. Mutations leading to an altered amino acid charge were mapped mainly to the variable regions but excluding the V3 loop. Structural modeling suggested that the modified residues were clustering and localized on the gp120 outer surface. Results also revealed that end-stage viruses displayed enhanced ability to associate with cells independently of CD4 and CCR5 expression. The net charge of gp120 also correlated with the CD4 count at time of virus isolation, virus attachment ability, replicative capacity, enhanced infectivity and reduced sensitivity to several entry inhibitors. Thus, after AIDS onset these features may evolve, in an opportunistic manner, and result in the emergence of HIV-1 R5 variants with enhanced pathogenic properties.

Results

Analysis of sequentially obtained R5 env sequences

To examine the molecular evolution of the HIV-1 R5 envelope glycoproteins during progressive disease, from the chronic phase to end-stage disease, we analyzed 48 *env* sequences (GenBank: EF600067–EF600114). These sequences were obtained from R5 primary isolates sequentially obtained before and after AIDS onset in six patients (Table 1). To determine the evolutionary relationships between the selected *env* sequences, maximum likelihood phylogenetic trees were constructed. Sequences from each patient clustered

Table 1
Patient clinical status, CD4 count, time to/from AIDS diagnosis and virus coreceptor use

Patient[a]	Isolate	CD4[b] count	Months[c] to AIDS	Clinical status	Coreceptor[d] use
G	1228	260	−9	Chronic asympt.	CCR5
	4481	5	+26	End-stage AIDS	CCR5
H	624	290	−27	Chronic asympt.	CCR5
	3899	6	+6	End-stage AIDS	CCR5
I	5013	140	−30	Chronic asympt.	CCR5
	8616	90	+11	End-stage AIDS	CCR5
J	1372	220	−11	Chronic asympt.	CCR5
	5714	20	+20	End-stage AIDS	CCR5
M	668	750	−54	Chronic asympt.	CCR5
	7363	20	+20	End-stage AIDS	CCR5
R	6322	200	−2	Chronic asympt.	CCR3+CCR5
	8004	9	+16	End-stage AIDS	CCR3+CCR5

[a] Patient code according to Jansson et al. (1999).
[b] $CD4^+$ T cells/μl at time of virus isolation.
[c] Time point of virus isolation related to months before and after AIDS diagnosis.
[d] Coreceptor use determined by infection of U87.CD4 and GHOST (3) coreceptor indicator cell lines expressing CCR2b, CCR3, CCR5, CXCR4, CXCR6 or BOB (Jansson et al., 1999).

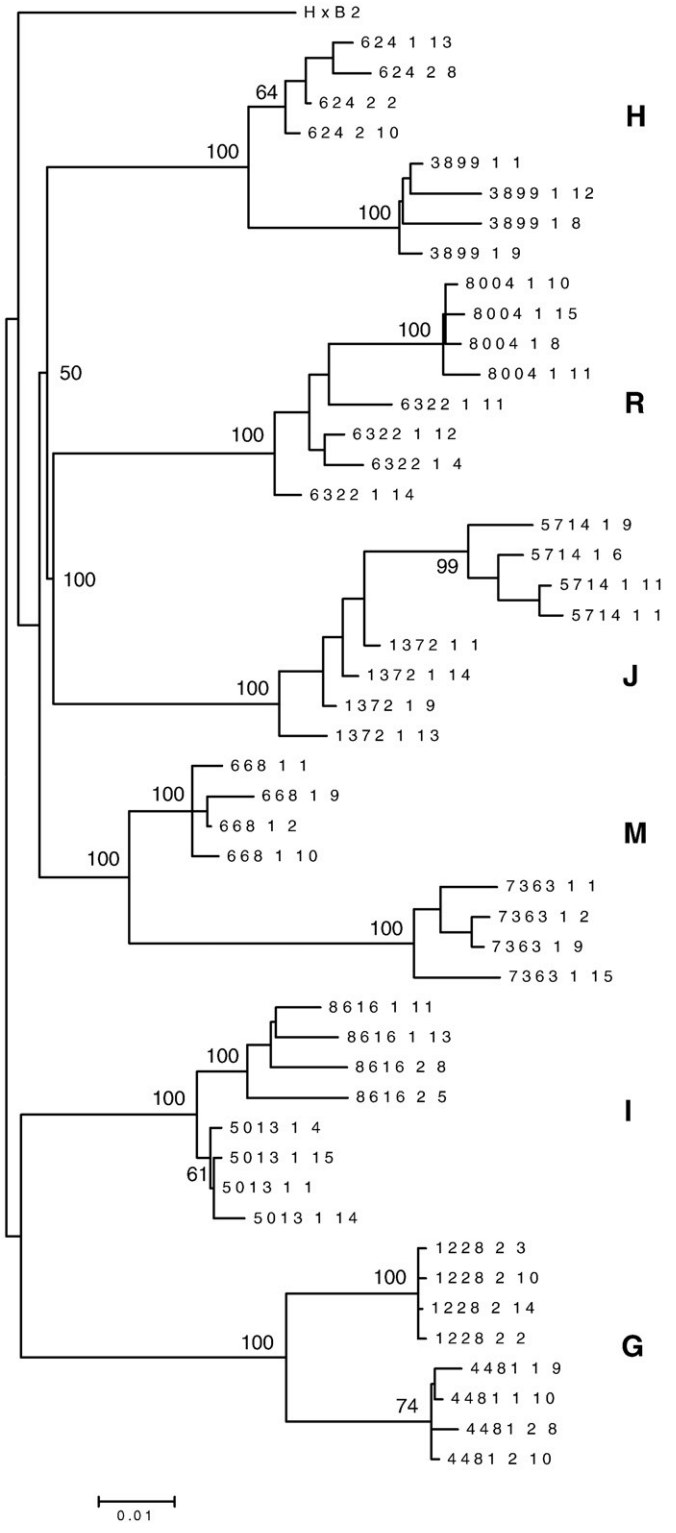

Fig. 1. Evolutionary relationships of *env* sequences encoding gp160 obtained from chronic and end-stage R5 viruses. Maximum likelihood trees were constructed using PAUP* (Sinauer Associates, Inc Publishers) with heuristic searches. Statistical support of the trees was obtained by 100 bootstrap replicates using the LUNARC computer cluster at Lunds University [http://www.lunarc.lu.se].

together and were separated from the sequences from all other patients by a bootstrap value of 100%. In addition, sequences from each isolation time point formed separate sub-clusters (Fig. 1). This phylogenetic analysis excludes contamination between patient specimens and/or isolation time points. In further analysis we examined the complete gp160 (Env) sequence as well as shorter segments, i.e. gp120, gp41 and gp120 variable loop regions.

Env of end-stage R5 viruses display increased net charge

The development of CXCR4-using viruses has been correlated to increased positive charge in specific Env regions (Hoffman and Doms, 1999). In the light of this we analyzed alterations in the charge of R5 Env sequences from primary isolates obtained before and after AIDS onset. We found that the gp160 sequences from end-stage disease of all patients displayed higher positive net charge when compared to corresponding sequences obtained prior to AIDS onset (Fig. 2a, $p=0.028$, Wilcoxon's matched pairs test). Mutations leading to an increase in positive charge were mapped to gp120, while no such pattern was observed for gp41 (Figs. 2b and c, $p=0.028$ and not significant respectively, Wilcoxon's matched pairs test). The exact location of amino acids with increased charge varied between the patients. However, we noted that mutations resulting in increased net charge mainly were localized in the variable gp120 regions (Fig. 2d), except the V3 loop, which was highly conserved when comparing Env sequences from chronic and end-stage R5 viruses. Nevertheless, three out of the six patients had end-stage R5 viruses with an increased charge in the regions flanking the gp120 V3 loop (Fig. 2d). In addition, it should be noted that among the gp120 V-regions an increased positive net charge was most frequent within the V2 and V4 regions since end-stage R5 Env sequences in a majority of the patients displayed increased positive charge within these regions (Fig. 2d and data not shown). To investigate the structural localization of the increased positive net charge within gp120 of end-stage R5 viruses we created molecular models of gp120 based on the Env sequences obtained before and after AIDS onset from patient G. The molecular models were created using the program SWISS-MODEL (Arnold et al., 2006), based on the homology of our Env sequences to the previously published crystal structure of HIV-1 gp120 (Huang et al., 2005). The molecular models comprise the core as well as the V3, V4 and V5 loops, but the V1 and V2 loops are excluded (Fig. 3a). As illustrated in Figs. 3b and c the molecular models indicate that, besides the observed increase in basicity within the V2 loop, most of the positively charged residues that were introduced following AIDS onset clustered on the surface of the gp120 structure, including the V4 loop, forming a novel basic region. It should be noted that the models suggest that most of the residues composing this relatively positively charged region protrude towards the solvent. Furthermore, most of this novel basic region is localized on the V4 loop, well separated from the previously described basic domain localized at the base of gp120 (that faces the target cell) (Kwong et al., 2000; Moulard et al., 2000) as well as the CD4 binding region (Wyatt and Sodroski, 1998) (Figs. 3b and c). It is also important to note that our model underestimates the overall gp120 charge differences since the observed positive shift in the V1V2 region net charge (Fig. 2d) is not displayed in the model. Accordingly, we conclude that gp120 of R5 virus variants emerging after AIDS onset undergoes substitutions that result in an increased net positive charge. These changes shift the amino acid net charge of gp120 and cluster to the V2 and V4 loops on an exposed region of the gp120 outer surface.

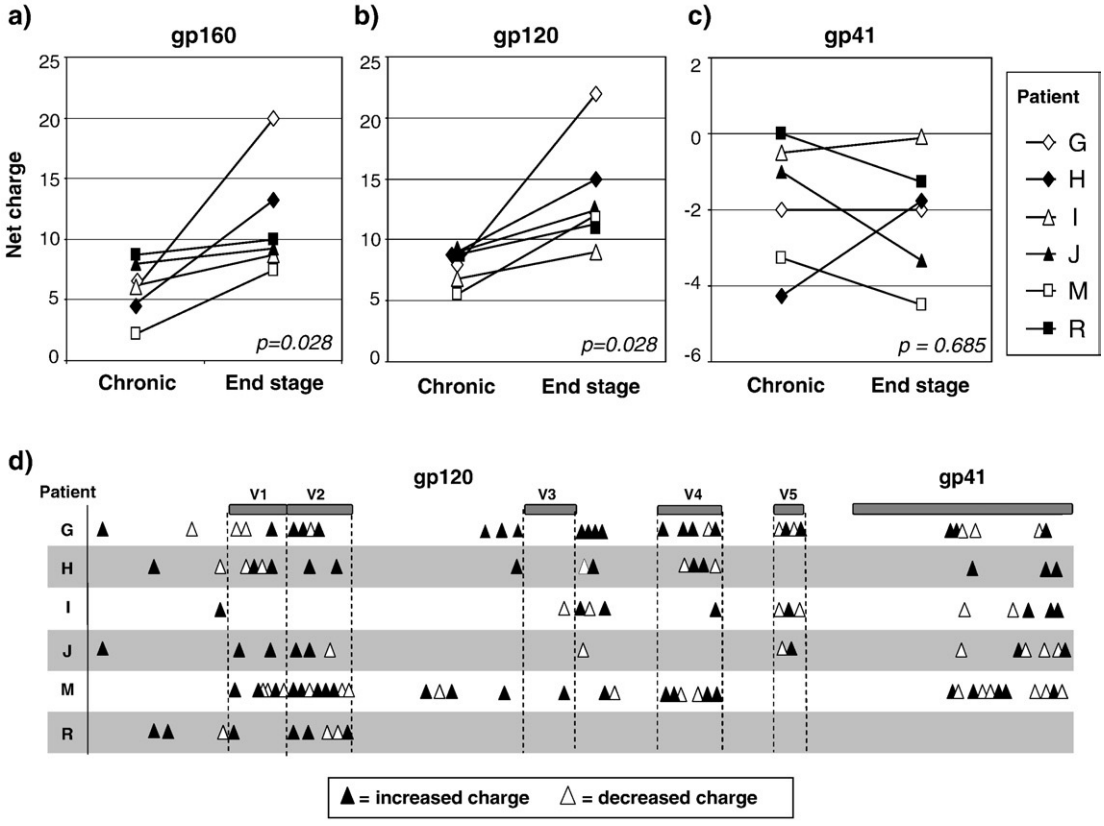

Fig. 2. Evolution and localization of charge modifications of HIV-1 R5 Env amino acid sequences during end-stage disease progression. Differences in net charge of a) gp160, b) gp120 and c) gp41 comparing the average charge of four R5 sequences per isolate obtained longitudinally at the asymptomatic chronic phase and after AIDS onset. d) Schematic view of localization of amino acid charge modifications within gp160 calculated from the average of four sequences per R5 isolate. Illustrated are amino acid positions where increased (filled triangles) or decreased (open triangles) positive charge have been noted comparing the end-stage Env sequences with corresponding chronic phase Env sequences.

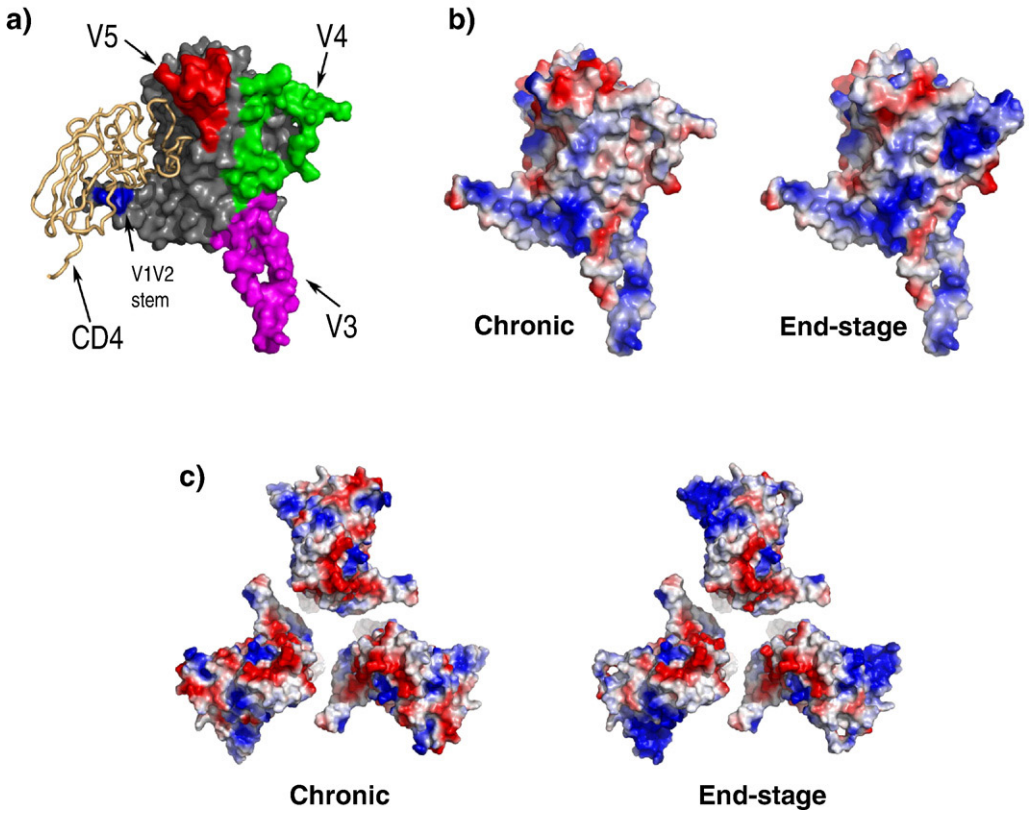

Fig. 3. Molecular models of monomeric and trimeric gp120 derived from sequentially obtained chronic and end-stage R5 viruses from patient G. a) Molecular surface representation of a model of monomeric gp120. A Cα tracing of the two N-terminal domains of CD4 is colored in yellow. The variable loops V1V2 (stem), V3, V4 and V5 are colored in blue, magenta, green and red, respectively. The rest of the surface of the molecule is colored grey. b) Electrostatic surfaces of chronic (left) versus end-stage (right) gp120. The electrostatic potential is shown at the solvent-accessible surface, which is colored according to the local electrostatic potential, ranging from dark blue (most positive) to deep red (most negative). c) Trimeric models of chronic (left) versus end-stage (right) gp120 derived from R5 Env clones from patient G. The trimer is depicted from the orientation of the viral membrane.

Increase in gp120 net positive charge correlates with patient immune status at time of R5 virus isolation

We next investigated whether the observed evolution in net charge was related to the immune status of the patients (Table 1). We compared the Env net charge with the CD4 count at time of virus isolation. The correlation analyses showed a strong inverse correlation between the CD4 count and the net charge of gp160 as well as gp120 (Figs. 4a and b) (p=0.00005, R=−0.90 and p=0.0006, R=−0.84, respectively according to Spearman rank correlation). In contrast, gp41 net charge did not correlate with CD4 count at time of virus isolation (Fig. 4c). These results suggest that *in vivo* evolution of the R5 HIV-1 gp120 during progressive disease may result in significant molecular changes such as increased positive net charge, which correlate with the immune status of the patient.

gp120 net charge correlates with properties related to viral fitness

We previously reported that R5 viruses that emerged after AIDS onset showed enhanced fitness, including elevated replicative capacity, increased infectivity and reduced sensitivity to several entry inhibitors (Gray et al., 2005; Jansson et al., 1996, 1999; Karlsson

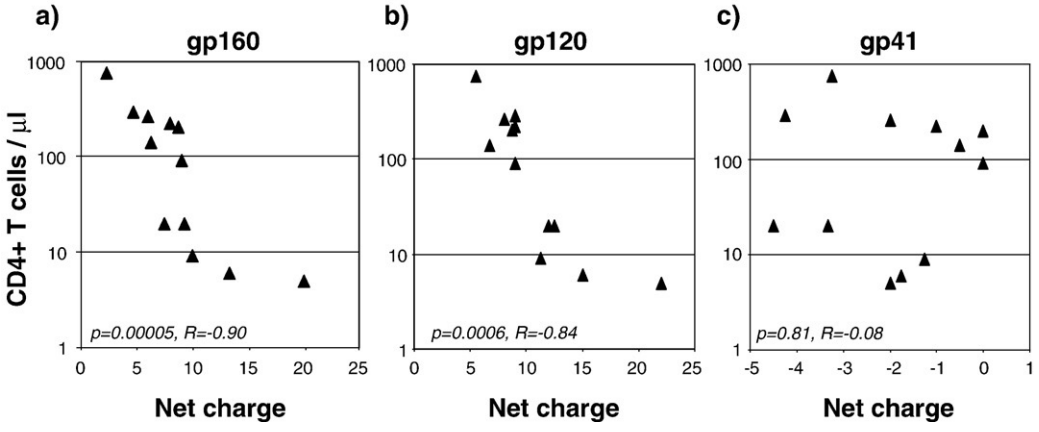

Fig. 4. Correlations between CD4 count at time of virus isolation and net charge of Env sequences. CD4 count in correlation to a) gp160, b) gp120 and c) gp41 net charge. Presented net charges are the average of four Env sequences per R5 isolate.

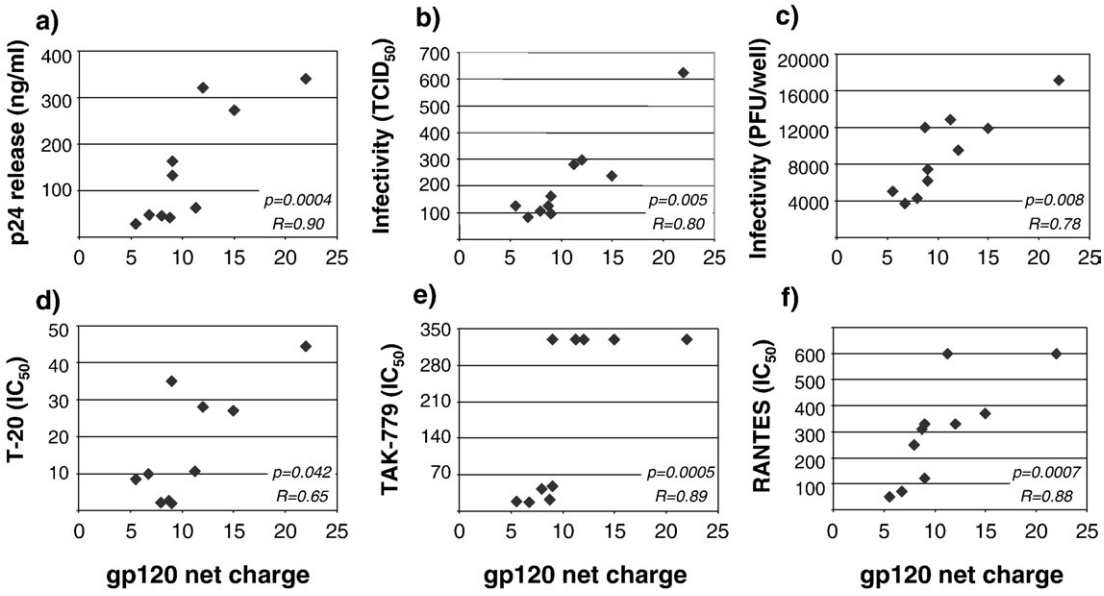

Fig. 5. gp120 net charge in relation to properties of viral fitness. Correlations between the gp120 net charge and a) replicative capacity in PBMC as assessed by p24 release, b) infectivity evaluated as TCID50 in PBMC, c) infectivity evaluated as plaque-forming units in U87.CD4.CCR5 cells, d) sensitivity to inhibition by fusion inhibitor T-20, e) sensitivity to inhibition by TAK-779 and f) sensitivity to inhibition by the natural CCR5 ligand RANTES.

et al., 2004; Repits et al., 2005; Sterjovski et al., 2007). To examine the underlying nature of these biological changes we investigated the relationship between molecular alterations leading to increased positive net charge in gp120 and markers of viral fitness. The analysis revealed clear correlations between the gp120 net charge and viral replicative capacity in PBMC, infectivity in PBMC and infectivity in U87.CD4.CCR5 ($p=0.0004$, $p=0.005$ and $p=0.008$ respectively according to Spearman rank correlation) (Figs. 5a–c). The net charge of gp120 also correlated with R5 virus sensitivity to inhibition by three different entry inhibitors, the fusion inhibitor T-20, the CCR5 antagonist TAK-779, and the natural CCR5 ligand RANTES ($p=0.042$, $p=0.0005$ and $p=0.0007$ respectively according to Spearman rank correlation) (Figs. 5d–f). Taken together, these results imply that increased viral fitness is correlated to the net charge of gp120.

End-stage R5 virus displays enhanced attachment to both $CD4^+CCR5^+$ and $CD4^-CCR5^-$ cells

Next, we investigated if the observed molecular changes i.e. increased positive net charge at the outer surface of the gp120 crown, affect the ability of viruses to associate with target cells. We performed virus attachment assays where virus was allowed to attach to cells, that either expressed specific receptors, i.e. CD4 and CCR5, or not. The amount of cell bound virus was calculated as the % p24 antigen, out of added p24, that remained after incubation, washing and cell lysis. Our results showed that end-stage viruses had an increased ability to attach to $CD4^+CCR5^+$ cells when compared to the corresponding chronic viruses as assessed using two different cell lines (Fig. 6a) ($p=0.004$; Wilcoxon's matched pairs test). End-stage viruses also displayed enhanced attachment to CD4 and CCR5 negative cells (Fig. 6b) ($p=0.005$; Wilcoxon's matched pairs test). Furthermore, the enhanced cell attachment of end-stage viruses was noted both when virus inoculum was normalized to the same level of functional RT (Figs. 6a and b) as well as the p24 antigen content (data not shown). In addition, cell-attachment ability correlated to the net charge of gp160 (Figs. 6c and d). This was true for cells expressing CD4 and CCR5 as well as receptor negative cells ($p=0.002$, $R=0.81$ and $p=0.0005$, $R=0.85$ respectively, Spearman rank correlation). Similarly, the gp120 net charge tended to correlate with degree of R5 virus attachment to both receptor positive and negative cells (Figs. 6e and f) ($p=0.060$, $R=0.56$ and $p=0.077$, $R=0.53$ respectively, Spearman rank correlation). Thus, the results indicate that R5 variants with an enhanced ability to attach to cells, independent of specific receptor expression, may evolve at end-stage of disease, and this ability correlates with Env amino acid net charge.

Discussion

By analysis of multiple Env sequences from sequentially obtained HIV-1 R5 isolates this study reveals molecular rationales for *in vivo* evolution of the R5 phenotype during severe immunodeficiency. In our studies of patients who maintain HIV-1 viruses exclusively using CCR5 we show that virus variants expressing gp120 with increased positive net charge emerge at end-stage disease along with declining $CD4^+$ T cell counts. The mutations leading to increased positive net charge of gp120 were mapped to the surface of the protein and mainly to the V2 and V4 variable regions. We also demonstrate correlations between gp120 net charge and different parameters related to the fitness of HIV-1 R5 isolates.

Both our work and that of others have demonstrated an *in vivo* evolution of the R5 phenotype during disease progression in patients that maintain CCR5 restricted HIV-1 viruses (Gorry et al., 2005; Gray et al., 2005; Jansson et al., 1996, 1999; Karlsson et al., 2004; Koning et al., 2003; Kwa et al., 2003; Repits et al., 2005; Sterjovski et al., 2007). R5 virus variants with altered biological properties, such as increased resistance to inhibition by CCR5 ligands and other entry inhibitors, may evolve during disease progression (Gray et al., 2005; Jansson et al., 1996, 1999; Karlsson et al., 2004; Koning et al., 2003; Kwa et al., 2003; Sterjovski et al., 2007; Sterjovski et al., 2006). The R5 variants emerging during disease progression also display enhanced cytopathicity and increased infectivity along with altered quantitative and qualitative demands on target cell receptors and enhanced sensitivity to neutralizing antibodies (Gray et al., 2005; Karlsson et al., 2004; Kwa et al., 2003; Repits et al., 2005; Sterjovski et al., 2007).

Our analysis of Env sequences from longitudinally obtained isolates revealed that gp120 from R5 isolates obtained at the end-stage of the disease display a higher net charge compared to viruses isolated at the chronic stage of HIV-1 disease. The mutations leading to increased charge were predominantly located in the variable regions of gp120, and most commonly in the V2 and V4 regions. In

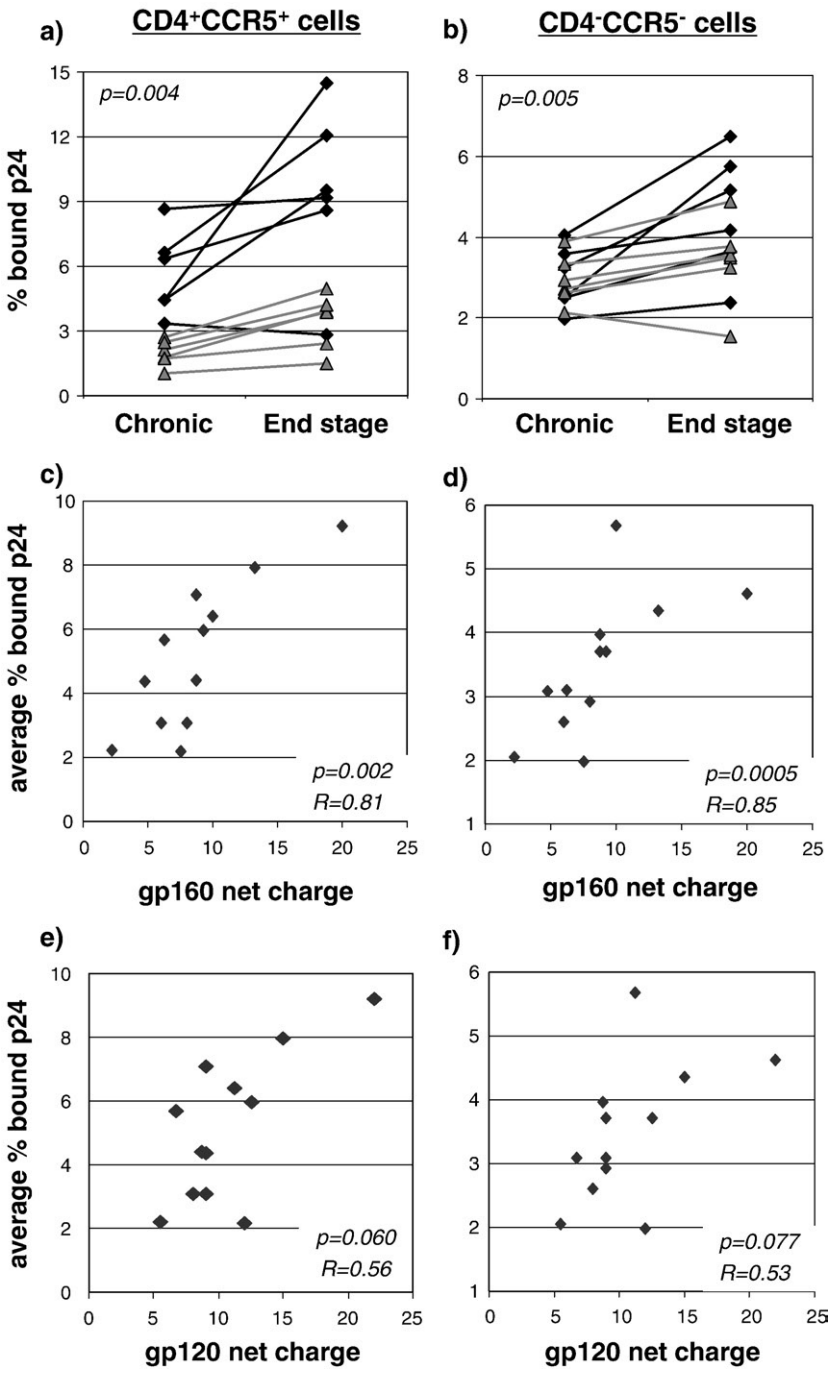

Fig. 6. Attachment of chronic and end-stage R5 viruses to $CD4^+CCR5^+$ and $CD4^-CCR5^-$ cells. Results are presented as % p24 of chronic and end-stage R5 viruses bound to a) $CD4^+CCR5^+$ cells; black diamonds = Cf2.CD4.CCR5 and gray triangles = NP-2.CD4.CCR5, or b) $CD4^-CCR5^-$ cells; black lines = 293T and grey lines = NP-2wt. Correlations between average % p24 bound to c) and e) $CD4^+CCR5^+$ cells or d) and f) $CD4^-CCR5^-$ cells and c) and d) gp160 and e) and f) gp120 net charge.

contrast, the charge of the V3 loop, which in many previous studies has been shown to be an important region for receptor interactions (Fouchier et al., 1992; Hwang et al., 1991), was conserved between all paired chronic and end-stage R5 *env* sequences. These findings suggest that changes in the net charge of the V3 loop may not be favored by CCR5-restricted viruses within patients that maintain exclusive R5 virus populations throughout the entire disease course. This is also in accordance with studies demonstrating that an increased V3 charge is indicative of a shift from CCR5- to CXCR4-use (Fouchier et al., 1992; Hoffman and Doms, 1999; Hwang et al., 1991).

The variable regions of gp120 are flexible loops protruding from the main body of the Env trimer, and are involved in receptor binding (Huang et al., 2005; Kwong et al., 1998). It is therefore reasonable to assume that the variable regions of gp120 are important in the initial contact between the virus and the target cell. Since the surface of the target cell as well as the overall virus surface are negatively charged the electrostatic repulsion must be overcome for successful virus binding. Comparing the V3-loop charge of non-syncytium inducing and syncytium inducing viruses it was previously hypothesized that increased positive charge of gp120 resulted in an initial enhanced interaction between virus- and target cell membranes, as a result of reduced repulsion (Callahan, 1994). Also, a recently proposed physical model of the initial steps of retrovirus infection suggests that the initial force for virus adsorption

is provided by non-specific electrostatic interactions (Davis et al., 2004). To counteract the electrostatic repulsion between membranes and aid virus adsorption a cationic polymer such as polybrene might be added to *in vitro* cultures (Davis et al., 2002). We previously reported that R5 isolates from end-stage disease do not benefit from such cationic assistance upon infection of PBMC (Repits et al., 2005). An overall increased positive net charge of the outermost parts of gp120 might provide these viruses an increased ability for non-specific adherence to the cell surface by reduced electrostatic repulsion between the viral and cell membranes. This may also explain why R5 viruses emerging at end-stage disease are less dependent on cationic assistance for target cell binding and entry.

Further support for the evolution of R5 viruses with enhanced adherence capacity can be derived from our observation that end-stage R5 viruses have an increased ability to attach to cells when compared to corresponding isolates obtained prior to AIDS onset. Interestingly, end-stage viruses had an elevated ability to attach to cells as compared to chronic-stage viruses, which was independent of receptor expression. This ability was furthermore shown to correlate to the net charge of gp160. Interestingly, the correlation between virus cell-attachment ability and net positive charge was stronger for gp160 than for gp120. Thus, it is possible that the charge of certain amino acid residues within gp41 may contribute to this viral property, even though cell-attachment ability was not correlated with the net charge of gp41 when analyzed separately (data not shown). Hence, these end-stage R5 viruses exhibit an unspecific adherence trait, which could be explained by the increased positive charge of the Env surface. Enhanced Env net charge may also account for our recent report on more promiscuous use of the CCR5 receptor by end-stage R5 viruses, as assessed by broadened chimeric receptor use (Karlsson et al., 2004).

In a parallel study we noted that R5 virus variants emerging following AIDS onset also display reduced numbers of potential N-linked glycosylation sites (PNGS) in the V2 and V4 regions (Borggren et al., 2008). Since glycans not only are bulky, but also negatively charged (Le Doux et al., 1996) loss of glycans may additionally contribute to the elevation of the overall Env charge and thus facilitate and enhance virus–cell interactions. Furthermore, loss of glycans may reduce solubility of the glycoproteins, and one potential mechanism to compensate for the reduced solubility might be to increase the net charge, and the hydrophilic properties, of the gp120 backbone. Thus, the observed increased basicity within the gp120 V2 and V4 regions may facilitate loss of glycans, which in turn might result in a more open pre-triggered Env structure. Interestingly, this positively charged region does not correspond to the CD4-binding region (Wyatt et al., 1998). Furthermore, this basic region was localized away from the previously described conserved basic region of the gp120 trimer that faces away from the virus, towards the target cell membrane (Kwong et al., 2000; Moulard et al., 2000).

Even if the molecular models suggest that the novel basic region within gp120 does not overlap with the CD4 binding site, a shift in the electrostatic potential that enlarge the basic surface of gp120 along with loss of glycans may render these viruses more fusogenic. A basic surface that does not comprise the CD4 binding site, nor the V3 loop, but conserved parts of the coreceptor binding site within gp120 have been identified and implicated in tropism and sensitivity of HIV-1 to polyanions (Moulard et al., 2000). Thus, we believe that the impact of altered gp120 charge and glycosylation patterns for HIV-1 entry mechanisms merits further investigations.

We also demonstrate a clear inverse correlation between the gp120 net charge and the immune status of the patient, as assessed by numbers of $CD4^+$ T cells at time of virus isolation. Further support for Env changes during the progressive loss of immunological competence was derived from calculations of dN/dS ratios. Both in gp120 and in gp41 these dN/dS ratios were found to be lower than 1.0, (data not shown) suggesting a comparatively low overall selection pressure for amino acid change in Env during progressive disease, which would be in agreement with previous studies (Williamson et al., 2005). However, despite the fact that the average positive Darwinian selection pressure for amino acid change was low, we clearly showed that amino acids in specific gp120 regions evolved towards higher charge. We believe that these changes may evolve as a result of diminished immune pressure. Thus, our data suggest that decreased strength of the host immunity may serve as a selection force at end-stage HIV infection, akin to the selection towards consensus sequences that has been reported in CTL epitopes when HIV is released from HLA-specific targeting during HIV transmission (Leslie et al., 2004). It is tempting to draw parallels between R5 viruses at the end-stage of the disease and those evolving in the environment of a primary HIV-1 infection. Hence, even though increased fitness may not be the result of the same viral properties, we believe that the selection mechanisms resulting in enhanced fitness could be comparable in the acute- and end-stages of the disease when a potent immune response is lacking. However, it is possible that reduced availability of target cells and altered receptor density also could contribute to the selection of viruses with increased fitness and altered Env structures (van Opijnen and Berkhout, 2005).

In the present study we report that along with declining $CD4^+$ T cell counts, mutations in gp120 result in increased positive charge of the protein surface and that these sequence changes correlate well with the viral fitness of the R5 viruses from which they originate. In support of this observation we have in a different set of R5 isolates, cross-sectionally obtained, also noted higher gp120 net charge in R5 isolates obtained after AIDS onset (Gorry and Sterjovski, unpublished data). We believe that the enlarged basic surface of gp120 in end-stage R5 HIV-1 may enhance non-specific electrostatic interactions between viral and cell membranes and aid adsorption of these viruses onto target cells. Thus, we propose a new mechanism that HIV-1 may use for the gain of viral fitness, which in turn could contribute to the pathogenicity of end-stage HIV-1 R5 viruses.

Materials and methods

Patients and virus isolates

Studied HIV-1 isolates were obtained from six patients selected from a larger cohort of homo- and bisexual men attending the South Hospital, Stockholm, Sweden (Table 1) (Karlsson et al., 1991; Karlsson et al., 1994). The selection was made on the basis of our previous finding that in patients that maintain R5 viruses throughout the course of the disease, R5 viruses with enhanced fitness and reduced sensitivity to RANTES and entry inhibitors may appear with progression to AIDS (Jansson et al., 1996, 1999; Repits et al., 2005). Four of these patients (G, I, J and R) received antiretroviral monotherapy (AZT or ddI). Isolations were made sequentially, at the chronic stage when the patients were clinically asymptomatic and after progression to AIDS. Virus stocks were generated by passaging virus isolates in PHA-stimulated (Boule) peripheral blood mononuclear cells (PBMC) from healthy donors. The R5 phenotype was determined by infection of the coreceptor indicator cell lines GHOST and U87 (Jansson et al., 1999). Isolates from patient R (6322 and 8004, see Table 1) displayed the ability to use both CCR5 and CCR3 in the indicator cell lines. However, since these isolates did not replicate in PBMC carrying the homozygous CCR5 Δ32 genotype (Jansson et al., 1999), they were classified being of R5 phenotype.

Generation of full-length env clones

Genomic DNA was extracted from PBMC infected with the HIV-1 R5 isolates seven days post infection, using a DNeasy DNA extraction kit (Qiagen) according to the manufacturer's protocol. HIV-1 *env* genes were amplified from genomic DNA using Expand high fidelity DNA polymerase and nested PCR approach as described previously (Gray et

al., 2006; Ohagen et al., 2003). The outer primers were Env1A and Env1M (Gao et al., 1996) and the inner primers were Env-KpnI and Env-BamHI (He et al., 1997) which amplifies a 2.1 kb fragment of HIV-1 *env* corresponding to nucleotides 6348 to 8478 of HxB2 and spans unique KpnI and BamHI restriction sites. PCR was performed with an initial denaturation step of 94 °C for 2 min, followed by 29 cycles of 95 °C for 15 s, 60 °C for 30 s, and 72 °C for 2 min, and a final extension of 72 °C for 7 min. During the last 20 cycles the extension time was increased by an additional 5 s per cycle. PCR product DNA was purified over a column using High Pure PCR Product Purification Kit (Roche) and cloned into the pSVIIIenv expression plasmid (Gao et al., 1996; Ohagen et al., 2003) by replacement of the 2.1 kb KpnI to BamHI HxB2 *env* fragment. Thus, the cloned *env* fragments contain the entire gp160 coding region except for 36 amino acids at the N-terminus and 105 amino acids at the C-terminus, which in the pSVIII plasmid derived from HxB2.

Sequence analysis of env clones

The pSVIIIenv plasmid was used as template for sequence analysis of the *env* gene and from each R5 isolate four clones were selected according to functionality in a single round entry assay described previously (Gorry et al., 2005; Gray et al., 2006). A set of 7 forward; F1EnvJR (5′-G/CAGAAAGAGCAGAAGACAGTGGCAATGA-3′), F2EnvJR (5′-GTCTATTATGGGGTACCTGTGTGG-3′), F3EnvJR (5′-GTGTACCCA-CAGACCCCAACCCACAAG-3′), F4EnvJR (5′-ACAATGC/TACACATGGAAT-TAA/GGCCA-3¢), F5EnvJR (5′-TTTAATTGTGGAGGGGAATTTTTCT-3′), F6EnvJR (5′-GTGGGAATAGGAGCTATGTTCCTTGGG-3′), F7EnvJR (5′-TATCAAAC/TTGGCTGTGGTATATAA-3′) and 8 reverse primers; R1EnvJR (5′-CTATCTGTCCCCTCAGCTACTGCTA-3′), R2EnvJR (5′-GCT-AAGAATCCATCCACT-AATCGT-3′), R3EnvJR (5′-CCTGCCTAACTCTATT-CAC-3′), R4EnvJR (5′-TTCAATTAG/AGGTGTATATTAAGCCTGTG-3′), R5EnvJR (5′-GCCCCAGACTGTGAGTTGCA-ACAGATG-3′), R6EnvJR (5′-GATGGGAGGGGCATACAT-3′), R7EnvJR (5′-CAGCAGTTGAGTT-GATACTACTGG-3′), R8EnvJR (5′-TTTAGCATCTGATGCACAAAATAG-3′) spanning the entire gp160 region and the ABI prism BigDye Terminator sequencing kit (Perkin Elmer) were used in the sequencing reaction. Sequence analysis was performed at the SWEGENE Centre of Genomic Ecology at Lund University. The sequenced segments were assembled to a contig sequence using the ContigExpress of VectorNTI Advance 10 software (Invitrogen). Sequences were aligned using ClustalX (Xia and Xie, 2001) followed by manual editing in GeneDoc [http://www.psc.edu/biomed/genedoc]. In order to rule out contamination between specimens a maximum likelihood tree containing sequences from all clones was constructed. The best-fitting nucleotide substitution model was identified with Modeltest (Posada and Crandall, 1998). Maximum likelihood trees were constructed using PAUP* (Sinauer Associates, Inc Publishers) with heuristic searches. Statistical support of the trees was obtained by 100 bootstrap replicates using the LUNARC computer cluster at Lunds University [http://www.lunarc.lu.se]. The gp160 sequences were analyzed as full-length segments and shorter regions i.e. gp120, gp41, gp120 variable regions. We defined the variable regions of gp120 as follows; V1 (nucleotide 6615–6692 in the HxB2 sequence), V2 (6693–6812), V3 loop (7110–7217), V4 (7377–7478) and V5 (7596–7637). The net charge of the sequences was calculated with each lysine (K) and arginine (R) contributing +1 and each aspartic acid (D) and glutamine (E) contributing −1. All presented charges were calculated as the average of four sequences per isolate. The charge difference at specific positions within gp160 was compared between end stage and chronic stage AIDS R5 isolates and ranged accordingly from −2 (four clones with basic aa replaced by four clones with acidic aa) to +2 (four clones with acidic aa replaced by four clones with basic aa). Phylogenetic analysis was performed using MEGA version 3.1 (Kumar et al., 2001). Pairwise nucleotide distances were computed using MEGA 3.1 under the Tamura–Nei nucleotide substitution model with gamma distributed rates among sites (gamma parameter α=0.5) and pairwise deletions.

Molecular modeling of chronic- and end-stage gp120

The molecular models of the gp120 monomers were created on the basis of their sequence homology to previously solved crystal structures of gp120, using the SWISS-MODEL protein modeling server (Guex and Peitsch, 1997). The crystal structure of gp120 in complex with CD4 and the X5 antibody ((Huang et al., 2005); pdb code 2B4C) was used as template for the creation of preliminary models of chronic and end-stage gp120. Fragments of the gp120 models, mainly from loop domains, were rebuilt according to secondary structure alignment. The molecular models of the trimeric gp120 were based on the previously published model of a trimeric gp120 (Posada and Crandall, 1998), kindly provided by Dr Peter D. Kwong and Dr Marie Pancera. The models of monomeric gp120 were superposed on each of the components of the trimer. The coordinates of all models will be provided upon request.

Virus cell-attachment assay

The ability of the studied viruses to attach to cells expressing the specific receptors, CD4 and CCR5, as well as unspecific binding to cells not expressing these receptors was tested. For this purpose we used NP-2 and Cf2th cells expressing CD4 and CCR5, in addition to NP-2wt and 293T cells being negative for CD4 and CCR5 expression. All cells were cultured in DMEM supplemented with 10% FCS (vol/vol), 0.1 μg/ml Streptomycin and 0.1 U/ml Penicillin. For selection of CD4 and CCR5 in NP-2 cells, 500 μg/ml Neomycin and 1 μg/ml Puromycin were added. For selection of CD4 and CCR5 in Cf2th/CD4^{+}CCR5^{+} cells 0.5 mg/ml G418 and 0.1 mg/ml hygromycin were added. Cells were seeded 1 day prior to the addition of virus. The concentration of functional RT has been shown to be a more accurate measurement of infectious virions compared to the p24 content (Corrigan et al., 1998; Malmsten et al., 2003; Marozsan et al., 2004). To avoid bias we tested in parallel the inoculum virus normalized to the same level of functional RT (2 or 5 ng/ml) and p24 content (10 ng/ml). 150 μl virus was allowed to attach for 3 h at 37 °C and there after the cells were extensively washed in PBS and resuspended in 100 μl lysis buffer (0.5% [vol/vol] NP-40; 0.5% [wt/vol] sodium deoxycholate; 50 mM NaCl; 25 mM Tris–HCl [pH 8.0]; 10 mM EDTA, 5 mM benzamidine HCl; and a cocktail of protease inhibitors). The level of virus attachment was analyzed by calculating % p24 antigen, out of added p24, that remained after incubation, washing and cell lysis using a p24 antigen ELISA (BioMérieux) according to the manufacturers' instructions.

Virus infectivity and replication assays

The infectivity and the replicative capacity of the studied HIV-1 R5 isolates were analyzed as described (Repits et al., 2005). In brief, infectivity was analyzed by determination of 50% tissue culture infectious dose (TCID50) in donor PBMC and plaque-forming units (PFU)/ml in U87.CD4.CCR5 cells in inoculum virus normalized for functional reverse tranciptase (RT) activity. Replicative capacity was evaluated by the analysis of p24 antigen release in cultures of donor PBMC infected with RT normalized R5 isolates.

Entry inhibitor sensitivity assay

The sensitivity of the HIV-1 R5 isolates to entry inhibitors was analyzed as described (Repits et al., 2005). In brief, donor PBMC were infected by R5 viruses in the presence of dilutions of CCR5-ligand RANTES, small molecule CCR5 antagonist TAK-779, and fusion inhibitor T-20. Sensitivity to the entry inhibitors was then evaluated

as 50% inhibitory concentrations calculated from the release of p24 antigen from control cultures infected in the absence of inhibitors.

Statistical analysis

For statistical analysis we used the Statistica software version 7. The non-parametric Spearman rank correlation was used for the analysis of correlations, while at comparisons between chronic and end-stage Env sequences and virus properties Wilcoxon's matched pairs test was used.

Acknowledgments

We thank Dr Joseph Sodroski for providing the pSVIIIenv expression plasmid and Cf2th-CD4/CCR5 cells, Dr Hiroo Hoshino for the NP-2 cell lines, Dr Daniel Littman for U87.CD4.CCR5 cell line, Dr Peter D Kwong and Dr Marie Pancera for molecular models and Hannes Uchtenhagen for suggestions on the manuscript. T20 fusion inhibitor from Roche and TAK-779 were obtained through the NIH AIDS Research and Reference Reagent Program, Division of AIDS, NIAD, NIH. DNA sequencing was performed at the SWEGENE Centre of Genomic Ecology at Lund University supported by the Knut and Alice Wallenberg Foundation through the SWEGENE consortium. The work was supported by grants provided to MJ from the Swedish Research Council and to MJ and EMF from the Swedish International Development Agency/Department for Research Cooperation (Sida/SAREC). Grants were also provided by the Magn. Bergvall's Foundation, the Physicians Against AIDS Research Foundation, Clas Groschinskys Foundation, the Royal Physiographic Society in Lund, Sweden. JR was given a travel grant from the Solander Foundation for a six month visit to the laboratory of PRG. PRG was supported in part by a grant from the Australian National Health and Medical Research Council (NHMRC) (433915). JS and LG were supported by Australian NHMRC Dora Lush Biomedical Postgraduate Research Scholarships. PRG is the recipient of an Australian NHMCR R. Douglas Wright Biomedical Career Development Award.

References

Arnold, K., Bordoli, L., Kopp, J., Schwede, T., 2006. The SWISS-MODEL workspace: a web-based environment for protein structure homology modelling. Bioinformatics 22 (2), 195–201.

Bjorndal, A., Deng, H., Jansson, M., Fiore, J.R., Colognesi, C., Karlsson, A., Albert, J., Scarlatti, G., Littman, D.R., Fenyo, E.M., 1997. Coreceptor usage of primary human immunodeficiency virus type 1 isolates varies according to biological phenotype. J. Virol. 71 (10), 7478–7487.

Borggren, M., Repits, J., Kuylenstierna, C., Sterjovski, J., Churchill, M.J., Purcell, D.F.J., Karlsson, A., Albert, J., Gorry, P.R., Jansson, M., 2008. Evolution of DC-SIGN use revealed by fitness studies of R5 HIV-1 variants emerging during AIDS progression. Retrovirology 5, 28.

Callahan, L., 1994. HIV-1 virion-cell interactions: an electrostatic model of pathogenicity and syncytium formation. AIDS Res. Hum. Retroviruses 10 (3), 231–233.

Corrigan, G.E., Al-Khalili, L., Malmsten, A., Thorstensson, R., Fenyo, E.M., Kallander, C.F., Gronowitz, J.S., 1998. Differences in reverse transcriptase activity versus p24 antigen detection in cell culture, when comparing a homogeneous group of HIV type 1 subtype B viruses with a heterogeneous group of divergent strains. AIDS. Res. Hum. Retroviruses 14 (4), 347–352.

Davis, H.E., Morgan, J.R., Yarmush, M.L., 2002. Polybrene increases retrovirus gene transfer efficiency by enhancing receptor-independent virus adsorption on target cell membranes. Biophys. Chem. 97 (2–3), 159–172.

Davis, H.E., Rosinski, M., Morgan, J.R., Yarmush, M.L., 2004. Charged polymers modulate retrovirus transduction via membrane charge neutralization and virus aggregation. Biophys. J. 86 (2), 1234–1242.

de Roda Husman, A.M., van Rij, R.P., Blaak, H., Broersen, S., Schuitemaker, H., 1999. Adaptation to promiscuous usage of chemokine receptors is not a prerequisite for human immunodeficiency virus type 1 disease progression. J. Infect. Dis. 180 (4), 1106–1115.

Fouchier, R.A., Groenink, M., Kootstra, N.A., Tersmette, M., Huisman, H.G., Miedema, F., Schuitemaker, H., 1992. Phenotype-associated sequence variation in the third variable domain of the human immunodeficiency virus type 1 gp120 molecule. J. Virol. 66 (5), 3183–3187.

Gao, F., Morrison, S.G., Robertson, D.L., Thornton, C.L., Craig, S., Karlsson, G., Sodroski, J., Morgado, M., Galvao-Castro, B., von Briesen, H., Beddows, S., Weber, J., Sharp, P.M., Shaw, G.M., Hahn, B.H., 1996. Molecular cloning and analysis of functional envelope genes from human immunodeficiency virus type 1 sequence subtypes A through G. The WHO and NIAID Networks for HIV Isolation and Characterization. J. Virol. 70 (3), 1651–1667.

Gorry, P.R., Churchill, M., Crowe, S.M., Cunningham, A.L., Gabuzda, D., 2005. Pathogenesis of macrophage tropic HIV-1. Curr. HIV Res. 3 (1), 53–60.

Gray, L., Sterjovski, J., Churchill, M., Ellery, P., Nasr, N., Lewin, S.R., Crowe, S.M., Wesselingh, S.L., Cunningham, A.L., Gorry, P.R., 2005. Uncoupling coreceptor usage of human immunodeficiency virus type 1 (HIV-1) from macrophage tropism reveals biological properties of CCR5-restricted HIV-1 isolates from patients with acquired immunodeficiency syndrome. Virology 337 (2), 384–398.

Gray, L., Churchill, M.J., Keane, N., Sterjovski, J., Ellett, A.M., Purcell, D.F., Poumbourios, P., Kol, C., Wang, B., Saksena, N.K., Wesselingh, S.L., Price, P., French, M., Gabuzda, D., Gorry, P.R., 2006. Genetic and functional analysis of R5X4 human immunodeficiency virus type 1 envelope glycoproteins derived from two individuals homozygous for the CCR5delta32 allele. J. Virol. 80 (7), 3684–3691.

Guex, N., Peitsch, M.C., 1997. SWISS-MODEL and the Swiss-PdbViewer: an environment for comparative protein modeling. Electrophoresis 18 (15), 2714–2723.

Hahn, B.H., Gonda, M.A., Shaw, G.M., Popovic, M., Hoxie, J.A., Gallo, R.C., Wong-Staal, F., 1985. Genomic diversity of the acquired immune deficiency syndrome virus HTLV-III: different viruses exhibit greatest divergence in their envelope genes. Proc. Natl. Acad. Sci. U. S. A. 82 (14), 4813–4817.

He, J., Chen, Y., Farzan, M., Choe, H., Ohagen, A., Gartner, S., Busciglio, J., Yang, X., Hofmann, W., Newman, W., Mackay, C.R., Sodroski, J., Gabuzda, D., 1997. CCR3 and CCR5 are co-receptors for HIV-1 infection of microglia. Nature 385 (6617), 645–649.

Hoffman, T.L., Doms, R.W., 1999. HIV-1 envelope determinants for cell tropism and chemokine receptor use. Mol. Membr. Biol. 16 (1), 57–65.

Huang, C.C., Tang, M., Zhang, M.Y., Majeed, S., Montabana, E., Stanfield, R.L., Dimitrov, D.S., Korber, B., Sodroski, J., Wilson, I.A., Wyatt, R., Kwong, P.D., 2005. Structure of a V3-containing HIV-1 gp120 core. Science 310 (5750), 1025–1028.

Hwang, S.S., Boyle, T.J., Lyerly, H.K., Cullen, B.R., 1991. Identification of the envelope V3 loop as the primary determinant of cell tropism in HIV-1. Science 253 (5015), 71–74.

Jansson, M., Popovic, M., Karlsson, A., Cocchi, F., Rossi, P., Albert, J., Wigzell, H., 1996. Sensitivity to inhibition by beta-chemokines correlates with biological phenotypes of primary HIV-1 isolates. Proc. Natl. Acad. Sci. U. S. A. 93 (26), 15382–15387.

Jansson, M., Backstrom, E., Bjorndal, A., Holmberg, V., Rossi, P., Fenyo, E.M., Popovic, M., Albert, J., Wigzell, H., 1999. Coreceptor usage and RANTES sensitivity of non-syncytium-inducing HIV-1 isolates obtained from patients with AIDS. J. Hum. Virol. 2 (6), 325–338.

Karlsson, A., Bratt, G., Von Krogh, G., Morfeldt-Manson, L., Bottiger, B., Sandstrom, E., 1991. A prospective study of 115 initially asymptomatic HIV infected gay men in Stockholm, Sweden. Scand. J. Infect. Dis. 23 (4), 431–441.

Karlsson, A., Parsmyr, K., Aperia, K., Sandstrom, E., Fenyo, E.M., Albert, J., 1994. MT-2 cell tropism of human immunodeficiency virus type 1 isolates as a marker for response to treatment and development of drug resistance. J. Infect. Dis. 170 (6), 1367–1375.

Karlsson, I., Antonsson, L., Shi, Y., Oberg, M., Karlsson, A., Albert, J., Olde, B., Owman, C., Jansson, M., Fenyo, E.M., 2004. Coevolution of RANTES sensitivity and mode of CCR5 receptor use by human immunodeficiency virus type 1 of the R5 phenotype. J. Virol. 78 (21), 11807–11815.

Koning, F.A., Kwa, D., Boeser-Nunnink, B., Dekker, J., Vingerhoed, J., Hiemstra, H., Schuitemaker, H., 2003. Decreasing sensitivity to RANTES (regulated on activation, normally T cell-expressed and -secreted) neutralization of CC chemokine receptor 5-using, non-syncytium-inducing virus variants in the course of human immunodeficiency virus type 1 infection. J. Infect. Dis. 188 (6), 864–872.

Koot, M., Keet, I.P., Vos, A.H., de Goede, R.E., Roos, M.T., Coutinho, R.A., Miedema, F., Schellekens, P.T., Tersmette, M., 1993. Prognostic value of HIV-1 syncytium-inducing phenotype for rate of CD4+ cell depletion and progression to AIDS. Ann. Intern. Med. 118 (9), 681–688.

Kumar, S., Tamura, K., Jakobsen, I.B., Nei, M., 2001. MEGA2: molecular evolutionary genetics analysis software. Bioinformatics 17 (12), 1244–1245.

Kwa, D., Vingerhoed, J., Boeser, B., Schuitemaker, H., 2003. Increased in vitro cytopathicity of CC chemokine receptor 5-restricted human immunodeficiency virus type 1 primary isolates correlates with a progressive clinical course of infection. J. Infect. Dis. 187 (9), 1397–1403.

Kwong, P.D., Wyatt, R., Robinson, J., Sweet, R.W., Sodroski, J., Hendrickson, W.A., 1998. Structure of an HIV gp120 envelope glycoprotein in complex with the CD4 receptor and a neutralizing human antibody. Nature 393 (6686), 648–659.

Kwong, P.D., Wyatt, R., Sattentau, Q.J., Sodroski, J., Hendrickson, W.A., 2000. Oligomeric modeling and electrostatic analysis of the gp120 envelope glycoprotein of human immunodeficiency virus. J. Virol. 74 (4), 1961–1972.

Le Doux, J.M., Morgan, J.R., Snow, R.G., Yarmush, M.L., 1996. Proteoglycans secreted by packaging cell lines inhibit retrovirus infection. J. Virol. 70 (9), 6468–6473.

Leslie, A.J., Pfafferott, K.J., Chetty, P., Draenert, R., Addo, M.M., Feeney, M., Tang, Y., Holmes, E.C., Allen, T., Prado, J.G., Altfeld, M., Brander, C., Dixon, C., Ramduth, D., Jeena, P., Thomas, S.A., St John, A., Roach, T.A., Kupfer, B., Luzzi, G., Edwards, A., Taylor, G., Lyall, H., Tudor-Williams, G., Novelli, V., Martinez-Picado, J., Kiepiela, P., Walker, B.D., Goulder, P.J., 2004. HIV evolution: CTL escape mutation and reversion after transmission. Nat. Med. 10 (3), 282–289.

Malmsten, A., Shao, X.W., Aperia, K., Corrigan, G.E., Sandstrom, E., Kallander, C.F., Leitner, T., Gronowitz, J.S., 2003. HIV-1 viral load determination based on reverse transcriptase activity recovered from human plasma. J. Med. Virol. 71 (3), 347–359.

Mansky, L.M., Temin, H.M., 1995. Lower in vivo mutation rate of human immunodeficiency virus type 1 than that predicted from the fidelity of purified reverse transcriptase. J. Virol. 69 (8), 5087–5094.

Marozsan, A.J., Fraundorf, E., Abraha, A., Baird, H., Moore, D., Troyer, R., Nankja, I., Arts, E.J., 2004. Relationships between infectious titer, capsid protein levels, and reverse

transcriptase activities of diverse human immunodeficiency virus type 1 isolates. J. Virol. 78 (20), 11130–11141.
Moulard, M., Lortat-Jacob, H., Mondor, I., Roca, G., Wyatt, R., Sodroski, J., Zhao, L., Olson, W., Kwong, P.D., Sattentau, Q.J., 2000. Selective interactions of polyanions with basic surfaces on human immunodeficiency virus type 1 gp120. J. Virol. 74 (4), 1948–1960.
Ohagen, A., Devitt, A., Kunstman, K.J., Gorry, P.R., Rose, P.P., Korber, B., Taylor, J., Levy, R., Murphy, R.L., Wolinsky, S.M., Gabuzda, D., 2003. Genetic and functional analysis of full-length human immunodeficiency virus type 1 env genes derived from brain and blood of patients with AIDS. J. Virol. 77 (22), 12336–12345.
Perelson, A.S., Neumann, A.U., Markowitz, M., Leonard, J.M., Ho, D.D., 1996. HIV-1 dynamics in vivo: virion clearance rate, infected cell life-span, and viral generation time. Science 271 (5255), 1582–1586.
Pierson, T.C., Doms, R.W., 2003. HIV-1 entry and its inhibition. Curr. Top. Microbiol. Immunol. 281, 1–27.
Posada, D., Crandall, K.A., 1998. MODELTEST: testing the model of DNA substitution. Bioinformatics 14 (9), 817–818.
Repits, J., Oberg, M., Esbjornsson, J., Medstrand, P., Karlsson, A., Albert, J., Fenyo, E.M., Jansson, M., 2005. Selection of human immunodeficiency virus type 1 R5 variants with augmented replicative capacity and reduced sensitivity to entry inhibitors during severe immunodeficiency. J. Gen. Virol. 86 (Pt 10), 2859–2869.
Sterjovski, J., Churchill, M.J., Wesselingh, S.L., Gorry, P.R., 2006. HIV-1 entry inhibitors: classes, applications and factors affecting potency. Curr. HIV Res. 4 (4), 387–400.
Sterjovski, J., Churchill, M.J., Ellett, A., Gray, L.R., Roche, M.J., Dunfee, R.L., Purcell, D.F., Saksena, N., Wang, B., Sonza, S., Wesselingh, S.L., Karlsson, I., Fenyo, E.M., Gabuzda, D., Cunningham, A.L., Gorry, P.R., 2007. Asn 362 in gp120 contributes to enhanced fusogenicity by CCR5-restricted HIV-1 envelope glycoprotein variants from patients with AIDS. Retrovirology 4, 89.
van't Wout, A.B., Kootstra, N.A., Mulder-Kampinga, G.A., Albrecht-van Lent, N., Scherpbier, H.J., Veenstra, J., Boer, K., Coutinho, R.A., Miedema, F., Schuitemaker, H., 1994. Macrophage-tropic variants initiate human immunodeficiency virus type 1 infection after sexual, parenteral, and vertical transmission. J. Clin. Invest. 94 (5), 2060–2067.
van Opijnen, T., Berkhout, B., 2005. The host environment drives HIV-1 fitness. Rev. Med. Virol. 15 (4), 219–233.
Williamson, S., Perry, S.M., Bustamante, C.D., Orive, M.E., Stearns, M.N., Kelly, J.K., 2005. A statistical characterization of consistent patterns of human immunodeficiency virus evolution within infected patients. Mol. Biol. Evol. 22 (3), 456–468.
Wyatt, R., Sodroski, J., 1998. The HIV-1 envelope glycoproteins: fusogens, antigens, and immunogens. Science 280 (5371), 1884–1888.
Wyatt, R., Kwong, P.D., Desjardins, E., Sweet, R.W., Robinson, J., Hendrickson, W.A., Sodroski, J.G., 1998. The antigenic structure of the HIV gp120 envelope glycoprotein. Nature 393 (6686), 705–711.
Xia, X., Xie, Z., 2001. DAMBE: software package for data analysis in molecular biology and evolution. J. Hered. 92 (4), 371–373.